



Research article

Fluorimetric detection of DNA methylation by cerium oxide nanoparticles for early cancer diagnosis

Mina Adampourezare^{a,*}, Behzad Nikzad^{a,**}, Mojtaba Amini^b, Nader Sheibani^c^a Research Center of Bioscience and Biotechnology, University of Tabriz, Tabriz, Iran^b Department of Inorganic Chemistry, Faculty of Chemistry, University of Tabriz, Tabriz, Iran^c Department of Ophthalmology and Visual Sciences, University of Wisconsin School of Medicine and Public Health, Madison WI 53705, USA

ARTICLE INFO

Keywords:

DNA methylation
Fluorescence
Nanobiosensor
CeO₂ nanoparticle

ABSTRACT

In this study, a very sensitive fluorescence nano-biosensor was developed using CeO₂ nanoparticles for the rapid detection of DNA methylation. The characteristics of CeO₂ nanoparticles were determined by transmission electron microscopy (TEM), scanning electron microscopy (SEM), energy dispersive spectroscopy (EDS), X-ray diffraction (XRD) spectroscopy, UV-visible spectroscopy, and fluorescence spectroscopy. The CeO₂ nanoparticles were reacted with a single-stranded DNA (ssDNA) probe, and then methylated and unmethylated target DNAs hybridized with an ssDNA probe, and the fluorescence emission was measured.

Upon adding the target unmethylated and methylated ssDNA, the fluorescence intensity increased in the linear range of concentration from 2×10^{-13} - 10^{-18} M. The limit of detection (LOD) was 1.597×10^{-6} M for methylated DNA and 1.043×10^{-6} M for unmethylated DNA. The fluorescence emission intensity of methylated sequences was higher than that of unmethylated sequences. The fabricated DNA nanobiosensor showed a fluorescence emission at 420 nm with an excitation wavelength of 280 nm. The impact of CeO₂ binding on methylated and unmethylated DNA was further demonstrated by agarose gel electrophoresis.

Finally, the actual sample analysis suggested that the nanobiosensor could have practical applications for detecting methylation in the human plasma samples.

1. Introduction

One of the most common epigenetic modifications is DNA methylation, which is the enzymatically catalyzed covalent addition (DNA methyltransferases) of a methyl (-CH₃) group from the methyl donor S-adenosylmethionine (SAM) to the 5' position carbon of the cytosine base within the CpG dinucleotide [1]. This heritable epigenetic modification without altering the coding sequence can lead to a change in gene expression [2–5]. Aberrant methylation at CpG islands of promotor of tumor suppressor genes can change gene transcription and directly result in gene silencing, which correlates with tumorigenesis [2,4,6]. The ability to detect DNA methylation in various clinical samples, such as serum and whole blood, suggests its potential application as a diagnostic tool (from early detection to post-therapy monitoring) [3,4,6–10]. Thus, it is crucial to optimize detection techniques for high sensitivity and specificity as well as high throughput [3].

* Corresponding author.

** Corresponding author.

E-mail addresses: adampourezare@gmail.com (M. Adampourezare), blsnikzad@yahoo.com (B. Nikzad).

Conventional methods for the detection of DNA methylation are mainly based on methylation-sensitive restriction enzyme digestion [11–13], affinity enrichment [14–16], and bisulfite treatment [17,18]. However, false-positive results caused by incomplete digestion [11–13], high cost and unstable antibodies [14–16], and incomplete conversion of unmethylated cytosine into uracil are disadvantages of these methods, respectively [17–20]. Recently, other methods are also used for the detection of DNA methylation, including (I) affinity enrichment techniques [21], (II) bisulfite treatment [22], and (III) sensitive restriction enzyme treatment [23–25]. These methods require specific chemical changes [26,27], which are costly and time-consuming. Thus, researchers are interested in using direct detection methods without chemical or enzyme treatments, as well as PCR methods to detect DNA methylation [28,29].

To overcome the limitations of traditional methods and the use of new evaluation methods, biosensor technology has been widely used to detect modifications and damages of biological molecules such as DNA, miRNA, and proteins [30,31].

Biosensors, as analytical devices for the detection of chemical species or events in biological samples, play a critical role in disease diagnosis as well as monitoring of disease progression and treatment efficacy [31]. Among various sensing methods, fluorescence technology is especially attractive due to its high sensitivity, better specificity, rapid detection, and low cost, easy operation and also its high sensitivity [32].

Fluorescence assays dominate some fields of biosensing because of high intrinsic sensitivity of this optical technique and the possibility of integration with receptors with high selectivity. In fluorescence detection, a specific wavelength of electromagnetic radiation excites fluorophore molecules and an optical transducer detects the intensity of shifted and emitted light. Three different approaches to bioassay target molecules using fluorescence methods including labeled, label free, and fluorescence resonance energy transfer (FRET) methods. The label free method is direct assay method of target molecules before and after the binding events. The labeled method is indirect detection method of target molecules by adding fluorescent labeling reagents such as organic dyes and nanoparticles (quantum dots, dye doped silica nanoparticles) [33].

Generally, an optical biosensor consists of three components, including a biological recognition element to recognize the analyte, a transducer element to convert the bio-recognition process into a measurable optical signal, and a detector element to display the imaging signal [34]. Nanomaterials can improve the biological recognition element's (biosensor's) efficiency by increasing their sensitivity and lowering their detection limits and providing rapid, low cost, and easy-to-use analytical tools. This advantage is due to their high specific surface area, which enables (bio)receptors to be immobilized on the surface in higher amounts [8–16,19].

Cerium oxide (CeO_2) is an essential n-type semiconductor metal oxide material with notable properties: high isoelectric point, biocompatibility, nontoxicity, wide band gap, and excellent electronic conductivity and stabilities [35]. Thus, this material has been widely investigated for its various applications as a biosensor [35–38], gas sensor [39], energy storage [40], and anticorrosion coat [41]. CeO_2 -NPs are used increasingly in nanotechnology and particularly in bioresearch. Cerium is the most abundant rare metal and shows high excitation energy. CeO_2 -NPs are a combination of Ce^{3+} and Ce^{4+} forms on the nanoparticle surface [42]. Thus, cerium oxide can exist in CeO_2 and Ce_2O_3 states [43,44]. The catalytic, optical, magnetic, and chemical properties of cerium are due to shielded 4f electrons [42,45,46]. The redox properties of cerium oxide are due to its unsaturation, which makes it unstable and affects its chemical reactivity and physicochemical properties [47–50].

Therefore, CeO_2 NPs possess multiple enzyme mimetic catalytic activities, including catalase (CAT), superoxide dismutase (SOD), phosphatase, peroxidase (POD), and mimetic properties, showing great potential to be used as a part of the optical biosensor for in vivo biomedical applications [51,52].

Recently, various studies have also been performed to apply the CeO_2 NPs for DNA biosensor applications. Pautler et al. [53] synthesized CeO_2 NPs for fluorometric biosensors to detect DNA. Nguyet et al. [54] designed a DNA biosensor based on CeO_2 -NR@Ppy nanocomposite to detect *Salmonella*. In this study, core-shell CeO_2 -NR@Ppy nanocomposite was prepared by in situ chemical oxidative polymerization of pyrrole monomer on CeO_2 -NRs, which provided a suitable platform for electrochemical DNA biosensor fabrication. The ss-DNA sequences onto nanocomposite coated-microelectrode were immobilized via the covalent attachment method. Cyclic voltammetry and electrochemical impedance spectroscopy were used to study DNA biosensor electrochemical responses. The linear range of concentration for this biosensor was 0.01–0.4 nM, and sensitivity was $593.7 \Omega \cdot \text{nM}^{-1} \cdot \text{cm}^{-2}$. The low limit of detection and limit of quantification for the DNA biosensor were 0.084 and 0.28 nM, respectively. Gao et al. [55] prepared a modified cerium oxide nanowire (CeO_2 NW) with carboxy fluorescein-labeled DNA for the determination of H_2O_2 . In this study, they concluded that 1D CeO_2 NW has higher DNA binding affinity and more efficient fluorescence quenching capability than that of zero-dimensional CeO_2 nanoparticles due to the electron transfer between CeO_2 NW and fluorophore-labeled DNA. By adding a high concentration of H_2O_2 , the absorbed DNA was released from CeO_2 NPs because of the stronger binding ability between H_2O_2 and Ce^{4+} than that between DNA and Ce^{4+} . Therefore, fluorescence signals were increased.

Nanoceria has also been extensively tested as an antioxidation agent and to stimulate the growth of stem cells [56–59]. Previous studies have used it for designing colorimetric biosensors [60,61]. Nanoceria has been reported to adsorb proteins based on electrostatic interactions [62]. In recent years, DNA has become a central molecule in bionanotechnology. Materials that adsorb DNA are interesting for developing biosensors, analytical separation, and gene delivery [63,64]. A native B-form double-stranded (ds) DNA is a highly negatively charged rod that can interact with surfaces via electrostatic forces. On the other hand, for single-stranded (ss) DNA, many intermolecular forces can take place, including hydrophobic strength, metal coordination, electrostatic force, hydrogen bonding, and aromatic stacking. Adsorbed DNA can regulate oxidase activity, presumably due to blocking substrate accessibility. Interestingly, nanoceria also has strong fluorescence quenching ability, providing further potential in biosensor development.

Analysis of circulating nucleic acids in bodily fluids, referred to as “liquid biopsies”, is rapidly gaining prominence. Studies have shown that cell-free DNA (cfDNA) has great potential in characterizing tumor status and heterogeneity, as well as the response to therapy and tumor recurrence. DNA methylation is an epigenetic modification that plays an important role in a broad range of

biological processes and diseases. It is well known that aberrant DNA methylation is generalizable across various samples and occurs early during the pathogenesis of cancer. Methylation patterns of cfDNA are also consistent with their originated cells or tissues. Systemic analysis of cfDNA methylation profiles has emerged as a promising approach for cancer detection and origin determination [65].

In this study, CeO₂ NPs were used as a fluorescent probe to fabricate a label-free DNA nanobiosensor to determine the DNA methylation of the APC gene. This was accomplished by adding an ssDNA probe to the solution containing cerium oxide nanoparticles (CeO₂ NPs). Thus, a simple and sensitive fluorometric method was used, based on the unique interactions of methylated and unmethylated DNA sequences with CeO₂ NPs, to detect methylation (Scheme 1). As shown in Scheme 1 and Fig. 3, the fluorescence emission was reduced by adding a pDNA sequence to cerium oxide nanocomposite. By adding unmethylated sequences to the pDNA and cerium oxide nanocomposite, the fluorescence emission was quenched, and by adding methylated sequences to the pDNA and cerium oxide nanocomposite, the fluorescence emission was increased.

2. Material and methods

2.1. Reagents and solutions

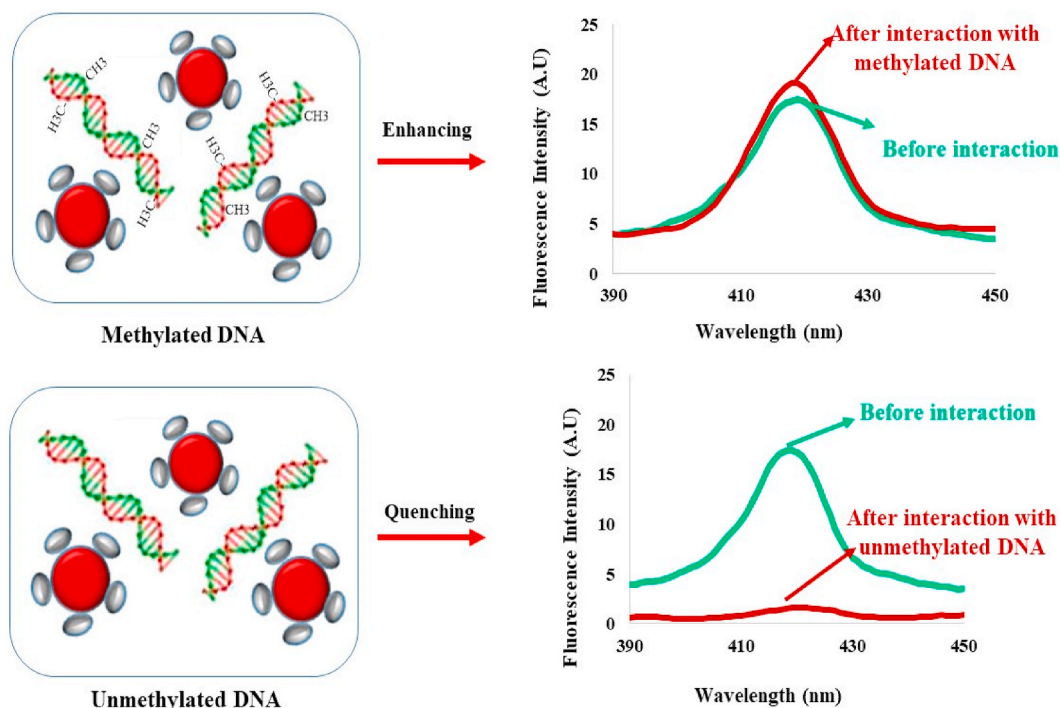
All chemicals were of analytical grade and used without further purification. Ultrapure water (deionized and doubly distilled) was used throughout the reaction. The sequence of 24 bp oligonucleotide designed based on the APC gene sequence was purchased from Shanghai General Biotech Co (Shanghai, China). The oligonucleotide sequences are as follows.

- Probe sequence (pDNA): TCCGCTCCCGACCCGCACTCCGC
- Complementary methylated sequence (target 1): GC(M)GGAGTGC(M)GGGTC(M)GGGAAGC(M)GGA
- Complementary methylated sequence (target 2) with one base mismatched: GC(M)GGAGTAC(M)GGGTC(M)GGGAAGC(M)GGA;
- Complementary unmethylated sequence (target 3): GCGGAGTCCGGGTCGGGAAGCGGA;
- Complementary unmethylated sequence (target 4) with one base mismatched: GCGGAGTACGGGTCGGGAAGCGGA;

All oligonucleotide stock solutions were prepared with TE Buffer (0.01 mol L⁻¹ Tris-HCl and 0.001 mol L⁻¹ EDTA; pH = 7.2) and kept in the refrigerator until use.

2.2. Apparatus

A PerkinElmer PF-750 spectrofluorometer (Japan) equipped with a 150 W xenon lamp as a source of excitation and a 1.0 cm quartz



Scheme 1. Schematic representation of the direct interaction of methylated and unmethylated DNA (6×10^{-13} M) with DNA nano-biosensor.

cell was used for fluorescence measurements. The spectral bandwidths of monochromators for excitation and emission were 5 nm. The size and shape of CeO₂ nanoparticles were studied by transmission electron microscopy (TEM) (Zeiss, EM10C, 80 KV, Germany). All experiments were performed at room temperature.

2.3. Synthesis of CeO₂ nanoparticle

CeO₂ nanoparticles were prepared using our previously reported method [66]. The Ce(OH)₄ particles were obtained by basifying an aqueous solution (10 cm³) of Ce(NO₃)₃·6H₂O (1.0 g) with NaOH solution (1.0 M; 10 ml). The obtained precipitate (Ce(OH)₄) was then mixed with urea (1.0 g) as a fuel, and the residual solid was calcined at 400 °C for 5 h.

2.4. Catalyst characterization

The X-ray diffraction (XRD) technique was employed to determine the phase of the synthesized nanoparticles. The XRD profile of the CeO₂ is presented in Fig. 1a, exhibiting conformity with the Fm3m cubic fluorite phase of CeO₂ (JCPDS file no. 34-0394) [67]. The absence of distinctive peaks originating from impurities in the XRD pattern of the prepared particles indicates the high purity of the CeO₂ nanoparticles. The presence of both cerium and oxygen in the CeO₂ sample was confirmed through energy-dispersive X-ray spectroscopy (EDXS), as depicted in Fig. 1b.

Scanning electron microscopy (SEM) and transmission electron microscopy (TEM) were utilized to conduct imaging of CeO₂ particles, as illustrated in Fig. 2. The SEM and TEM images revealed that the particles exhibited a nearly spherical shape, with dimensions ranging from approximately 50 to 80 nm.

2.5. Preparation of DNA nano biosensor

First, a solution of CeO₂ nanoparticles (100 μl) was prepared with a concentration of 1 mg ml⁻¹ in doubly distilled water. The ssDNA probe (2 μL of 10⁻¹³ M) was added to the microtube containing CeO₂ nanoparticles. The ssDNA probe was preheated at 90 °C for 2 min before use, and after reaching 50 °C, they were reacted with CeO₂ nanoparticles. The reaction mixture was then centrifuged at 1200 rpm for 10 min to mix and complete the interaction between CeO₂ nanoparticles and bases of the ssDNA probe (Fig. 3).

2.6. Fluorescence measurements

The hybridization reaction was performed by gently stirring at 37 °C and pH = 7.2. However, 4 μl of ssDNA target with 10⁻¹³ M concentration was denatured at 90 °C for 2 min and the temperature then was reduced to 50 °C [45,66]. The ssDNA target was then added to the microtube containing the prepared DNA nano-biosensor and was incubated at 37 °C for 40 min, as optimized hybridization time [68]. Fluorescence evaluation was carried out at excitation and emission wavelengths of 280 nm and 400–440 nm, respectively (Fig. 3).

Note: In performing each part of the test, we repeated the test at least three times and then obtained an average of the results and compared the average of the data and determined the standard error for each group of data and plotted the error bar.

3. Results and discussion

3.1. Interaction of CeO₂-NPs with ssDNA probe

Generally, surface groups such as carboxyl, carbonyl, epoxy, and hydroxyl and C, O, and H elements can participate in the

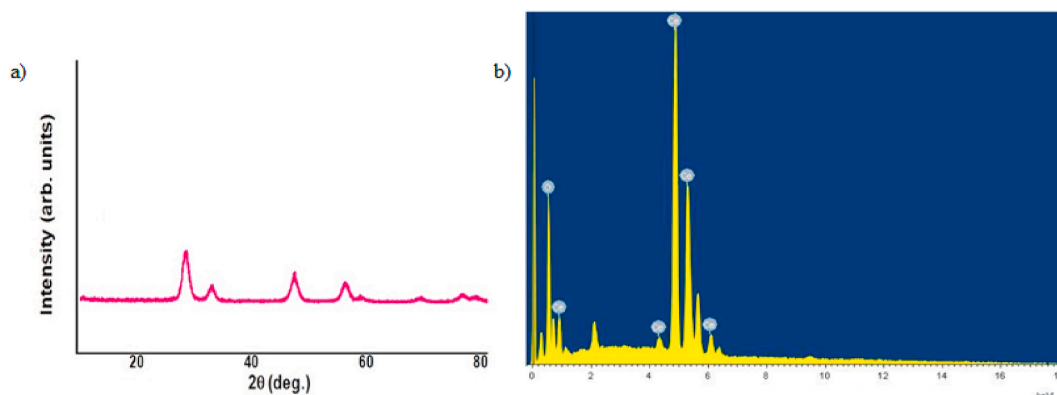


Fig. 1. a) XRD pattern; b) EDXS analysis of CeO₂ nanoparticles.

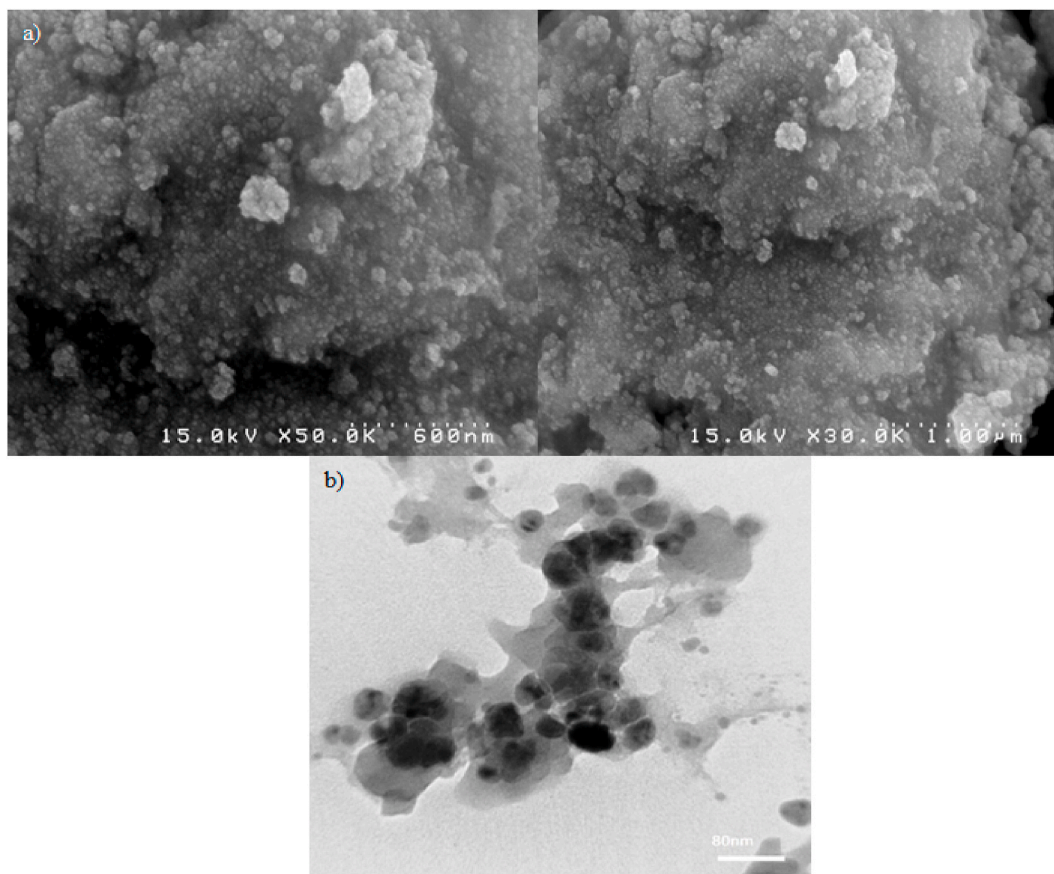


Fig. 2. a) SEM images; b) TEM image of CeO₂ nanoparticles.

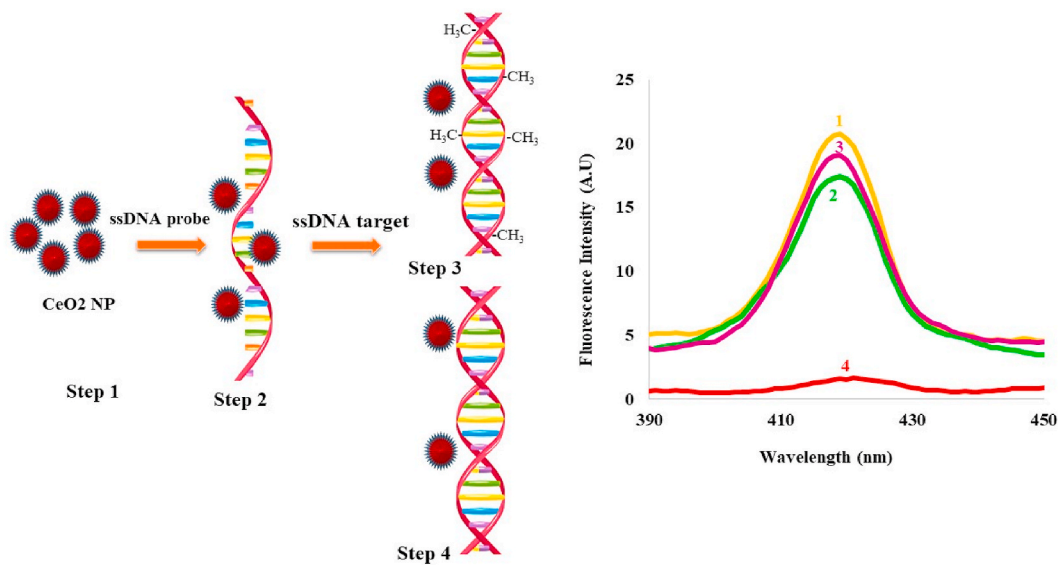


Fig. 3. Preparing steps of DNA nano-biosensor (steps 1,2) and its hybridization to methylated ssDNA target (step 3) and unmethylated ssDNA target (step 4).

formation of hydrogen and electrostatic bonds [69–73]. In addition, metal elements containing positive charge can participate in the formation of electrostatic adsorption and metal coordination. For example, Zhou et al. applied chitosan-modified CeO₂ nanorods to immobilize DNA probes onto the electrode surface through electrostatic adsorption and metal coordination [74].

The interaction of the ssDNA probe with CeO₂-NPs caused a sensitive quenching. To have a better understanding of the fluorescence quenching mechanism, different concentrations of ssDNA probes were reacted with CeO₂-NPs, and the Stern-Volmer curve was drawn. Fig. 4 shows that the increase in the concentration of the ssDNA probe caused a decrease in the emission intensity. The value of the linear equation with regression coefficient (R) was 0.5903. Thus, CeO₂-NPs and the ssDNA probe (phosphate, sugar groups, and bases) bind together and form a stable complex. According to the regression equation of the Stern-Volmer curve, $F_0/F = -0.6009x + 23.989$ (unit of C is M). Hence, we found that the ssDNA probe was located on the surface of CeO₂ NPs, which agrees with previously reported work [20].

3.2. Influence of ssDNA target sequences on fluorescence intensity

To prove the effect of hybridization on fluorescence intensity, the DNA nano-biosensor (CeO₂-NPs + pDNA) was titrated with different concentrations of methylated and unmethylated ssDNA targets under optimal conditions. The fluorescence emission intensity gradually decreased with the increased concentration of complementary methylated and unmethylated ssDNA targets from 10^{-18} to 2×10^{-13} M. The reduced values of fluorescence intensity for unmethylated ssDNA concentration were linear with a regression equation of $\Delta F = 1.5541C + 7.1923$ (unit of C is M), and the regression coefficient (R) of the linear curve was $R^2 = 0.986$. Also, the increased values of fluorescence intensity for methylated ssDNA concentration were linear with a regression equation of $\Delta F = 2.578C + 17.259$, and the regression coefficient (R) of the linear curve was $R^2 = 0.9492$. The detection limit was estimated at 1.043×10^{-6} M. It is possible that both complementary sequences exhibited the fluorescence response because CeO₂-NPs could bind to both hybridized DNA. However, a significant difference was noted since the emission intensity of different concentrations of methylated DNA was consistently higher than the emission intensity of different concentrations of unmethylated DNA (Figs. 5 and 6).

According to previous studies, single-stranded DNA is more effectively adsorbed by cerium nanoparticles than ds-DNA, is reflected by fluorescence quenching. Adsorption of DNA is possible not only by electrostatic interaction through the binding of its phosphate backbone to cerium oxide but also by Lewis acid-base interaction. Nanoceria is a strong and general fluorescence quencher. Adsorption of DNA blocks the surface access of substrate molecules and inhibits the oxidase activity of nanoceria [76,77]. On the other hand, Rafiei and colleagues [75] investigated the interaction of methylated and unmethylated DNA with GQD nanoparticles. They showed that DNA methylation affects not only the mechanism of DNA interaction with GQD but also the helix structure of DNA and changes the conformation of the DNA structure. So, changing the conformation of methylated DNA probably reduces its interaction with cerium oxide nanoparticles, which increases the fluorescence emission of cerium oxide nanoparticles.

Thus, the results indicated that developed DNA nanobiosensor can discriminate methylated DNA from unmethylated DNA. Table 1 compares the detection limit of the present study with previous studies. According to the results of last in Table 1 and by comparing the concentration range, detection limit, and structure of nanocomposites used in previous studies with the present study, it can be concluded that the detection limit and concentration range of current study is in accordance with the results of previous studies.

3.3. Effect of hybridization time on the fluorescence intensity of DNA nano-biosensor

To study the effect of hybridization time on the intensity of fluorescence emission after the hybridization of cerium oxide nanoparticles with a DNA probe, the intensity of fluorescence emission was evaluated at different times. It was observed that 40 min is the optimum reaction time. This was consistent with the observed hybridization time of 40 min. Thus, the reaction time of 40 min was chosen as the appropriate reaction time (Fig. 7).

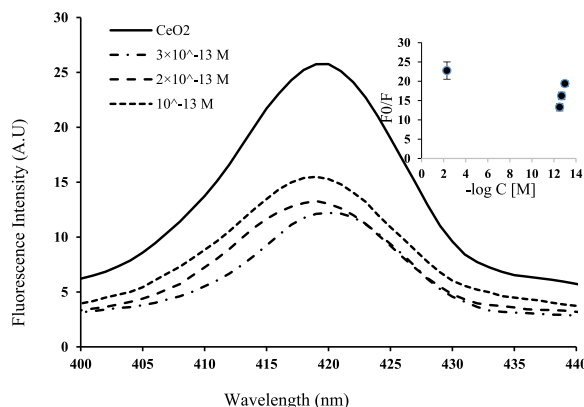


Fig. 4. A) Fluorescence spectra of fabricated DNA nano-biosensor (CeO₂-NPs + pDNA) reaction with various concentrations of pDNA (3×10^{-13} , 2×10^{-13} , 1×10^{-13} M), (CeO₂-NPs = 5×10^{-3} M).

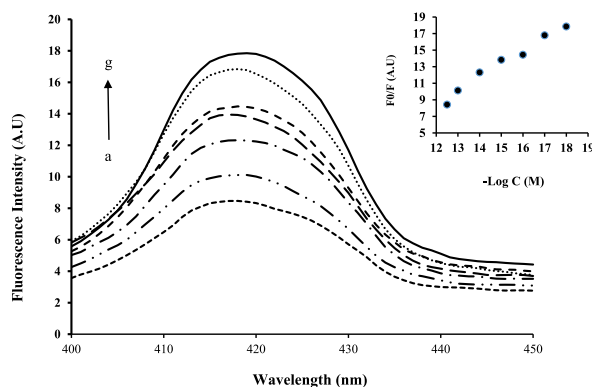


Fig. 5. (A) Fluorescence spectra of fabricated DNA nano-biosensor ($\text{CeO}_2\text{-NPs} + \text{pDNA}$) with the concentration of 10^{-13} M probe DNA and various concentrations of unmethylated ssDNA target sequences (2×10^{-13} , 10^{-13} , 10^{-14} , 10^{-15} , 10^{-16} , 10^{-17} , 10^{-18} M from “a” to “g” in order), and incubation time of 40 min.

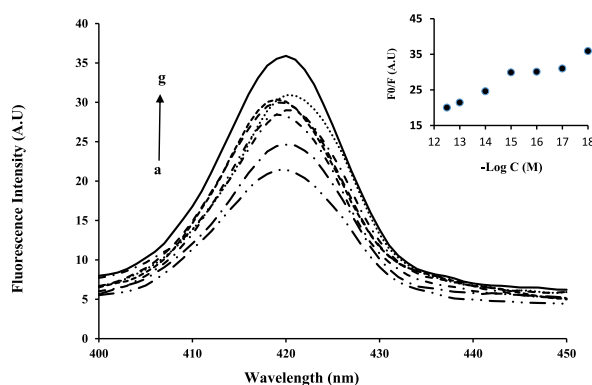


Fig. 6. (A) Fluorescence spectra of fabricated DNA nano-biosensor ($\text{CeO}_2\text{-NPs} + \text{pDNA}$) with the concentration of 10^{-13} M probe DNA and various concentrations of methylated ssDNA target sequences (2×10^{-13} , 1×10^{-13} , 10^{-13} , 10^{-14} , 10^{-15} , 10^{-16} , 10^{-17} , 10^{-18} M from a to g in order), and incubation time of 40 min.

Table 1

Comparison of LOD (limit of detection) of fluorescence biosensing strategies for DNA methylation detection.

Method	Gene	Nanomaterial	Linear range/M	Limit of detection (LOD)/M	Ref.
Labeled fluorescence	adenomatous polyposis coli (APC)	$\text{Fe}_3\text{O}_4/\text{Au}$ core/shell, Dipyrindamole	3.2×10^{-15} – 8.0×10^{-13} M	0.3×10^{-15} M	[76]
Label-free, fluorescence	APC	Graphene quantum dots (GQDs)	10.0×10^{-10} M to 10.0×10^{-6} M	73×10^{-6} M	[77]
Label-free, fluorescence	APC	thionine-based polymer	10^{-21} – 0.3×10^{-12} M	10^{-21} M	[78]
Label-free, fluorescence	APC	toluidine blue-based polymer	10^{-21} – 0.3×10^{-12} M	10^{-21} M	[79]
Label-free, fluorescence	APC	Thioglycolic acid (TGA)-capped CdTe quantum dots (QDs)	1.0×10^{-10} to 1.0×10^{-6} M	6.2×10^{-11} M	[75]
FAM-labeled, FRET	P53	gold nanoparticles (AuNPs)	5–100 pM	2.2 pM	[80]
Label-free, fluorescence	APC	CeO_2 NPs	2×10^{-13} – 10^{-18} M	1.597×10^{-6} M for methylated DNA and 1.043×10^{-6} M for unmethylated DNA	This report

3.4. Specificity and selectivity study of $\text{CeO}_2\text{-NPs}$

The specificity and selectivity of the $\text{CeO}_2\text{-NPs}$ were studied using hybridization of the $\text{CeO}_2\text{-NPs}$ with different oligonucleotide sequences including (A) unmethylated complementary sequence, (B) unmethylated sequence with one-base mismatched (in non-CpG sites), (C) methylated complementary sequence, (D) methylated complementary sequence with one-base mismatched (in non-CpG sites), with the same concentration (6×10^{-13} M) and the results were compared (Fig. 8). Fluorescence emission intensity for

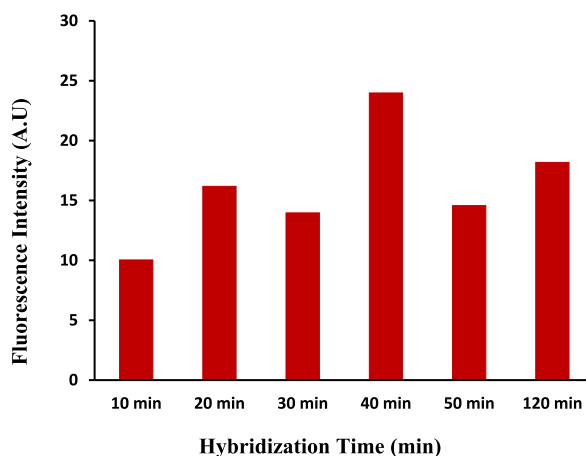


Fig. 7. Fluorescence intensity of CeO₂ NPs (concentration: 10⁻¹³ M) at different times.

hybridization with the unmethylated sequence was lower than methylated sequence. The fluorescence intensity of sequences containing one-base mismatch for methylated and unmethylated sequences was higher than that of entirely complementary sequences (one-base mismatch for methylated DNA = 14.2, methylated DNA = 14, one-base mismatch unmethylated sequences = 12, unmethylated sequences = 11.8). These results demonstrated the high selectivity of our DNA biosensor. We showed that a mismatch in the DNA sequence increased the fluorescence emission of both methylated and unmethylated DNA. Thus, partial hybridization affects fluorescence emission. Therefore, our DNA nano-biosensor has high specificity and sensitivity for detecting DNA damage.

3.5. Gel electrophoresis of DNA-CeO₂ Complexes

The interaction of CeO₂ nanoparticles with methylated and unmethylated DNA was assayed using agarose gel electrophoresis in Tris-HCl buffer solution (pH 7.2). The image of agarose gel electrophoresis demonstrated the interaction effect of CeO₂ on methylated and unmethylated DNA (Fig. 9). The intensity in the bands related to methylated sequences was higher than unmethylated sequences.

Different fluorescence emissions will appear as fluorescence emissions. Fig. 9 shows that the addition of CeO₂ to methylated and unmethylated DNA caused an increase in fluorescence emission in the electrophoresis assay. These results demonstrated that gel electrophoresis could distinguish methylated and unmethylated DNA sequences.

According to the results of previous researches in Table 1 and by comparing the concentration range, detection limit, and structure of nanocomposites used in previous studies with the present study, it can be concluded that the detection limit and concentration range of the current research is in accordance with the results of previous studies. We also provided a data set table to compare the present obtained results with the previous studies on methylation recognition by different nanoparticles. From the view of linear range and detection limit, our proposed method showed the priorities over the mentioned reports. This nanocomposite can identify methylated and unmethylated sequences and non-complementary sequences, and even sequences with a non-complementary base from each other. Its disadvantages include its high detection limit. Also, the different sequences identified by the fluorescence emission are very little different. In the studies carried out by other publications, the fluorescence of different identified sequences at a specific concentration has not been compared.

4. Conclusion

In this study, a fluorometric DNA nano-biosensor, based on cerium oxide molecules, was designed to detect DNA methylation. Cerium oxide nanoparticles were characterized using TEM and SEM microscopy, FTIR, and EDXS. This label-free fluorometric method could distinguish methylated from unmethylated sequences. Also, the presence of non-complementary nucleotides in the DNA sequence could be detected with this nanoparticle. Here, due to the critical role of the APC gene, part of the sequence of this gene was selected to evaluate the efficiency of our CeO₂-NPs. The results of fluorescence evaluations showed that the emission intensity of methylated DNAs was higher than that of unmethylated DNAs, and sequences containing non-complementary bases showed higher emission intensity. The gel electrophoresis results further confirmed the difference in fluorescence intensity of methylated and non-methylated sequences. In general, this designed nano-biosensor has high sensitivity and selectivity in detecting DNA methylation.

Additional information

No additional information is available for this paper.

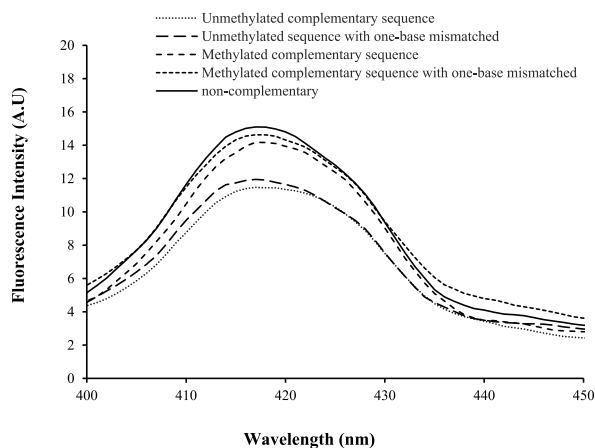


Fig. 8. Fluorescence spectra of CeO₂-NPs in the presence of different DNA sequences, including unmethylated complementary sequence, unmethylated sequence with a one-base mismatch (in non-CpG sites), methylated complementary sequence, methylated complementary sequence with a one-base mismatch (in non-CpG sites), and non-complementary sequence at same concentrations (6×10^{-13} M).

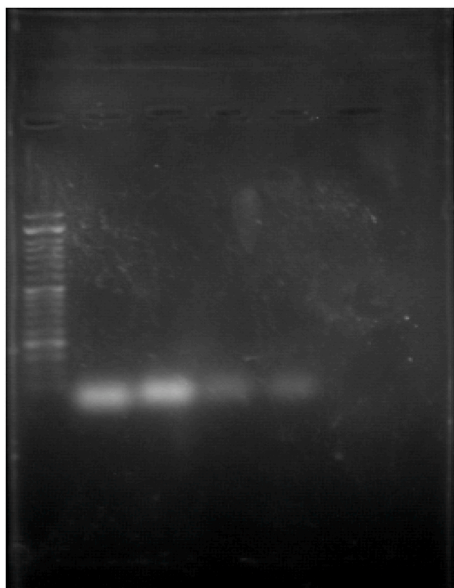


Fig. 9. Image of agarose gel electrophoresis of methylated and unmethylated DNA with addition CeO₂: 1: DNA ladder. 2,3: methylated DNA + CeO₂ 4,5: unmethylated DNA + CeO₂.

CRedit authorship contribution statement

Mina Adampourezare: Writing – review & editing, Writing – original draft, Supervision, Methodology, Investigation, Data curation, Conceptualization. **Behzad Nikzad:** Writing – review & editing. **Mojtaba Amini:** Writing – review & editing. **Nader Sheibani:** Writing – review & editing.

Declaration of competing interest

The authors declare the following financial interests/personal relationships which may be considered as potential competing interests.

Acknowledgments

The researchers thank the University of Tabriz for its support of this research.

References

- [1] M. Esteller, Epigenetics in Cancer, vol. 13, CRC Press, 2008, pp. 1148–1159.
- [2] A. Bird, DNA methylation patterns and epigenetic memory, *Genes Dev.* 16 (2002) 6–21.
- [3] P.W. Laird, The power and the promise of DNA methylation markers, *Nat. Rev. Cancer* 3 (2003) 253–266.
- [4] S.B. Baylin, J.E. Ohm, Epigenetic gene silencing in cancer - a mechanism for early oncogenic pathway addiction, *Nat. Rev. Cancer* 6 (2006) 107–116.
- [5] P.A. Jones, S.B. Baylin, The epigenomics of cancer, *Cell* 128 (2007) 683–692.
- [6] J.G. Herman, S.B. Baylin, N. Engl, Gene silencing in cancer in association with promoter hypermethylation, *J. Med.* 349 (2003) 2042–2054.
- [7] M. Esteller, L. Catusas, X. Matias-Guiu, G.L. Mutter, J. Prat, S.B. Baylin, J.G. Herman, hMLH1 promoter hypermethylation is an early event in human endometrial tumorigenesis, *Am. J. Pathol.* 155 (1999) 1767–1772.
- [8] M. Esteller, J. Garcia-Foncillas, E. Andion, S.N. Goodman, O.F. Hidalgo, V. Vanacllocha, Inactivation of the DNA-repair gene MGMT and the clinical response of gliomas to alkylating agents, *J. Med.* 343 (2000) 1350–1354.
- [9] S.D. Gore, S. Baylin, E. Sugar, H. Carraway, C.B. Miller, M. Carducci, M. Grever, O. Galm, T. Dausies, J.E. Karp, M.A. Rudek, M. Zhao, B.D. Smith, Combined DNA methyltransferase and histone deacetylase inhibition in the treatment of myeloid neoplasms, *Cancer Res.* 66 (2006) 6361–6369.
- [10] M.V. Brock, H.C. Hooker, E. Ota-Machida, Y. Han, M. Guo, S. Ames, S. Glöckner, S. Dna, Methylation markers and early recurrence in stage I Lung cancer, *J. Med.* 358 (2008) 1118–1128.
- [11] J.Y. Zhang, B.L. Xing, J.Z. Song, F. Zhang, C.Y. Nie, Associated analysis of DNA methylation for cancer detection using CCP-based FRET technique, *Anal. Chem.* 86 (2014) 346–350.
- [12] Q. Yang, Y. Dong, W. Wu, C. Zhu, Detection and differential diagnosis of colon cancer by a cumulative analysis of promoter methylation, *Nat. Commun.* 3 (2012) 1206.
- [13] M. Oda, J.L. Glass, R.F. Thompson, Y. Mo, E.N. Olivier, High-resolution genome-wide cytosine methylation profiling with simultaneous copy number analysis and optimization for limited cell numbers, *J. M. Nucleic Acids Res.* 37 (2009) 3829–3839.
- [14] R. Kurita, K. Arai, K. Nakamoto, D. Kato, O. Niwa, Determination of DNA methylation using electrochemiluminescence with surface accumulative coreactant, *Anal. Chem.* 84 (2012) 1799–1803.
- [15] Y. Hori, N. Otomura, A. Nishida, M. Nishiura, M. Umeno, Synthetic-molecule/protein hybrid probe with fluorogenic switch for live-cell imaging of DNA methylation, *J. Am. Chem. Soc.* 140 (2018) 1686–1690.
- [16] D. Hiraoka, W. Yoshida, K. Abe, H. Wakeda, K. Hata, K. Ikebukuro, Development of a method to measure DNA methylation levels by using methyl CpG-binding protein and luciferase-fused zinc finger protein, *Anal. Chem.* 84 (2012) 8259–8264.
- [17] P.W. Laird, Principles and challenges of genome-wide DNA methylation analysis, *Nat. Rev. Genet.* 11 (2010) 191–203.
- [18] J.G. Herman, J.R. Graff, S. Myohanen, B.D. Nelkin, S.B. Baylin, Methylation-specific PCR: a novel PCR assay for methylation status of CpG islands, *Proc. Natl. Acad. Sci. U. S. A.* 93 (1996) 9821–9826.
- [19] T. Ushijima, Detection and interpretation of altered methylation patterns in cancer cells, *T, Nat. Rev. Cancer* 5 (2005) 223–231.
- [20] S. Derks, M.H. Lentjes, D.M. Hellebrekers, A.P. de Bruine, J.G. Herman, Promoter CpG island methylation of RET predicts poor prognosis in stage II colorectal cancer patients, *M. Cell. Oncol* 26 (2004) 291–299.
- [21] M. Weber, J.J. Davies, D. Wittig, E.J. Oakeley, M. Haase, Chromosome-wide and promoter-specific analyses identify sites of differential DNA methylation in normal and transformed human cells, *Nat. Genet.* 37 (2005) 853–862.
- [22] A.P. Bird, Use of restriction enzymes to study eukaryotic DNA methylation: II. The symmetry of methylated sites supports semi-conservative copying of the methylation pattern, *J. Mol. Biol.* 118 (1978) 49–60.
- [23] M. Frommer, L.E. McDonald, D.S. Millar, A genomic sequencing protocol that yields a positive display of 5-methylcytosine residues in individual DNA strands, *Proc. Natl. Acad. Sci. U. S. A.* 89 (1992) 1827–1831.
- [24] M. Adampourezare, G. Dehghan, M. Hasanzadeh, M.A. Hosseinpoure Feizi, Application of lateral flow and microfluidic bio-assay and biosensing towards identification of DNA-methylation and cancer detection: recent progress and challenges in biomedicine, *Biomed. Pharmacother.* 141 (2021) 111845.
- [25] R.L. Mompalmer, V. Bovenzi, DNA methylation and cancer, *J. Cell. Physiol.* 183 (2000) 145–154.
- [26] S. Bareyt, T. Carell, Selective detection of 5-methylcytosine sites in DNA, *Angew. Chem. Int. Ed.* 47 (2008) 181–184.
- [27] T.A. Clark, X. Lu, K. Luong, Q. Dai, M. Boitano, S.W. Turner, C. He, J. Korch, Enhanced 5-methylcytosine detection in single-molecule, real-time sequencing via Tet1 oxidation, *BMC Biol.* 11 (2013) 4.
- [28] M. Dadmehr, M. Hosseini, S. Hosseinkhani, M.R. Ganjali, R. Sheikhejad, Label free colorimetric and fluorimetric direct detection of methylated DNA based on silver nanoclusters for cancer early diagnosis, *Biosens. Bioelectron.* 73 (2015) 108–113.
- [29] J.R. Lakowicz, B.R. Masters, Principles of fluorescence spectroscopy, *J. Biomed. Opt.* 13 (2008), 029901–029902.
- [30] C. Briones, M. Moreno, Applications of peptide nucleic acids (PNAs) and locked nucleic acids (LNAs) in biosensor development, *Anal. Bioanal. Chem.* 402 (2012) 3071–3089.
- [31] P. Li, G.-H. Lee, S.Y. Kim, S.Y. Kwon, H.R. Kim, S. Park, From diagnosis to treatment: recent advances in Patient-Friendly biosensors and Implantable devices, *ACS Nano* 15 (2021) 1960.
- [32] Z.L. Lei, B. Guo, 2D material-based optical biosensor: status and Prospect, *Adv. Sci.* 9 (2022) 2102924.
- [33] M. Adampourezare, M. Hasanzadeh, F. Seidi, Optical bio-sensing of DNA methylation analysis: an overview of recent progress and future prospects, *RSC Adv.* 12 (2022) 25786.
- [34] V. Nares, N. Lee, A Review on biosensors and recent development of nanostructured materials-enabled biosensors, *Sensors* 21 (2021) 1109.
- [35] A. Anees A. Ansari, P.R. Solanki, B.D. Malhotra, Sol-gel derived nanostructured cerium oxide film for glucose sensor, *Appl. Phys. Lett.* 92 (2008) 263901.
- [36] A. Kumar Yagati, T. Lee, J. Min, J.W. Choi, An enzymatic biosensor for hydrogen peroxide based on CeO₂ nanostructure electrodeposited on ITO surface, *Biosens. Bioelectron.* 47 (2013) 385–390.
- [37] Y. Zhai, Y. Zhang, F. Qin, X. Yao, An electrochemical DNA biosensor for evaluating the effect of mix anion in cellular fluid on the antioxidant activity of CeO₂ nanoparticles, *Biosens. Bioelectron.* 70 (2015) 130–136.
- [38] N.T. Nguyet, L.T. Hai Yen, V.V. Thu, H. Ian, T. Trung, P.H. Vuong, P.D. Tam, Highly sensitive DNA sensors based on cerium oxide nanorods, *J. Phys. Chem. Solids* 115 (2018) 18–28.
- [39] E. Laubender, N.B. Tanvir, O. Yurchenko, G. Urban, Nanocrystalline CeO₂ as room temperature sensing material for CO₂ in low power work function sensors, *Procedia Eng.* 120 (2015) 1058–1062.
- [40] R. Murugan, G. Ravi, R. Yuvakkumar, S. Rajendran, N. Maheswari, G. Muralidharan, Y. Hayakawa, Pure and Co doped CeO₂ nanostructure electrodes with enhanced electrochemical performance for energy storage applications, *Ceram. Int.* 43 (2017) 10494–10501.
- [41] A. Madhan Kumar, R. Suresh Babu, S. Ramakrishna, A.L.F. de Barros, Electrochemical synthesis and surface protection of polypyrrole-CeO₂ nanocomposite coatings on AA2024 alloy, *Synth. Met.* 234 (2017) 18–28.
- [42] A. Dhall, W. Self, Cerium oxide nanoparticles: a brief review of their synthesis methods and biomedical applications, *Antioxidants* 7 (8) (2018) 97.
- [43] C. Bouzigues, T. Gacoin, A. Alexandrou, Biological applications of rare-earth based nanoparticles, *ACS Nano* 5 (11) (2011) 8488–8505.
- [44] S. Tsunekawa, R. Sivamohan, S. Ito, A. Kasuya, T. Fukuda, Structural study on monosize CeO₂-x nano-particles, *Nanostruct. Mater.* 11 (1) (1999) 141–147.
- [45] M. Taguchi, S. Takami, T. Naka, T. Adschiri, Growth mechanism and surface chemical characteristics of dicarboxylic acid-modified CeO₂ nanocrystals produced in supercritical water: tailor-made water-soluble CeO₂ nanocrystals, *Cryst. Growth Des.* 9 (12) (2009) 5297–5303.
- [46] R.B. Kshiti, N. Vanya, T. Sarkar, R. Pratap, Cerium oxide nanoparticles: properties, biosynthesis and biomedical application, *RSC Adv.* 10 (2020) 27194.
- [47] J. Conesa, Computer modeling of surfaces and defects on cerium dioxide, *Surf. Sci.* 339 (1995) 337–352.
- [48] G.S. Herman, Characterization of surface defects on epitaxial CeO₂(001) films, *Surf. Sci.* 437 (1999) 207–214.

- [49] T. Suzuki, I. Kosacki, H.U. Anderson, P. Colomban, Electrical conductivity and lattice defects in nanocrystalline cerium oxide thin films, *J. Am. Ceram. Soc.* 84 (2004) 2007–2014.
- [50] F. Esch, S. Fabris, L. Zhou, T. Montini, C. Africh, P. Fornasiero, G. Comelli, R. Rosei, Electron localization determines defect formation on ceria substrates, *Science* 309 (2005) 752–755.
- [51] H. Wei, E. Wang, Nanomaterials with enzyme-like characteristics (nanozymes): next-generation artificial enzymes (II), *Chem. Soc. Rev.* 42 (2013) 6060.
- [52] F. Charbgoon, M. Ramezani, M. Darroudi, Bio-sensing applications of cerium oxide nanoparticles: Advantages and disadvantages, *Biosens. Bioelectron.* 96 (2017) 33.
- [53] R. Pautler, E.Y. Kelly, P.J. Jimmy Huang, J. Cao, B. Liu, J. Liu, Attaching DNA to nanoceria: Regulating oxidase activity and fluorescence quenching, *ACS Appl. Mater. Interfaces* 14 (2013) 6820–6825.
- [54] N.T. Nguyeta, L.T. Hai Yena, V.Y. Doana, N. Luong Hoanga, V.V. Thuc, H. Iana, T. Trungb, V.H. Phama, P.D. Tam, A label-free and highly sensitive DNA biosensor based on the core-shell structured CeO₂-NR@Ppy nanocomposite for *Salmonella* detection, *Mater. Sci. Eng. C* 96 (2019) 790–797.
- [55] W. Gao, X. Wei, X. Wang, G. Cui, Z. Liu, B. Tang, A competitive coordination-based CeO₂ nanowire–DNA nanosensor: fast and selective detection of hydrogen peroxide in living cells and in vivo, *Chem. Commun.* 52 (2016) 3643.
- [56] C. Menchon, R. Martín, N. Apostolova, V. Victor, Gold nanoparticles supported on nanoparticulate ceria as a powerful agent against intracellular oxidative stress, *Small* 8 (2012) 1895–1903.
- [57] C. Mandoli, F. Pagliari, S. Pagliari, G. Forte, Stem cell aligned growth induced by CeO₂ nanoparticles in PLGA scaffolds with improved bioactivity for regenerative medicine, *Adv. Funct. Mater.* 20 (2010) 1617–1624.
- [58] A.S. Karakoti, S. Singh, A. Kumar, M. Malinska, S.V.N.T. Kuchibhatla, K. Wozniak, W.T. Self, PEGylated nanoceria as radical scavenger with tunable redox chemistry, *J. Am. Chem. Soc.* 131 (2009) 14144–14145.
- [59] I. Celardo, J.Z. Pedersen, E. Traversa, L. Ghibelli, Pharmacological potential of cerium oxide nanoparticles, *Nanoscale* 3 (2011) 1411–1420.
- [60] M. Ornatka, E. Sharpe, D. Andreescu, S. Andreescu, Paper bioassay based on ceria nanoparticles as colorimetric probes, *Anal. Chem.* 83 (2011) 4273–4280.
- [61] E. Sharpe, T. Frasco, D. Andreescu, S. Andreescu, Portable ceria nanoparticle-based assay for rapid detection of food antioxidants (NanoCerac), *Analyst* 138 (2013) 249–262.
- [62] S. Patil, A. Sandberg, E. Heckert, W. Self, S. Seal, Protein adsorption and cellular uptake of cerium oxide nanoparticles as a function of zeta potential, *Biomaterials* 28 (2007) 4600–4607.
- [63] R.H. Yang, J.Y. Jin, Y. Chen, N. Shao, H.Z. Kang, Carbon nanotube-quenched fluorescent oligonucleotides: probes that fluoresce upon hybridization, *J. Am. Chem. Soc.* 130 (2008) 8351–8358.
- [64] K. Saha, S.S. Agasti, C. Kim, X. Li, V.M. Rotello, Gold nanoparticles in chemical and biological sensing, *Chem. Rev.* 112 (5) (2012) 2739–2779.
- [65] J. Huang, L. Wang, Cell-free DNA methylation profiling analysis—Technologies and Bioinformatics, *Cancers* 11 (2019) 1741.
- [66] G. Bülbül, A. Hayat, F. Mustafa, S. Andreescu, DNA assay based on nanoceria as fluorescence quenchers (NanoCeracQ DNA assay), *Sci. Rep.* 8 (2018) 1–9.
- [67] M. Amini, R. Hassandoost, M. Bagherzadeh, S. Gautam, K.H. Chae, Copper nanoparticles supported on CeO₂ as an efficient catalyst for click reactions of azides with alkynes, *Catal. Commun.* 85 (2016) 13–16.
- [68] Y. Zhang, Z. Wang, W. Jiang, A sensitive fluorimetric biosensor for detection of DNA hybridization based on Fe/Au core/shell nanoparticles, *Analyst* 136 (2011) 702–707.
- [69] I.L. Medintz, H.T. Uyeda, E.R. Goldman, H. Mattoussi, Quantum dot bioconjugates for imaging, labelling and sensing, *Nat. Mater.* 4 (2005) 435.
- [70] L. Sun, W. Wu, X. Wei, Recent advances in graphene quantum dots for sensing, *Mater. Today* 16 (2013) 433–442.
- [71] J. Shen, Y. Zhu, X. Yang, C. Li, Graphene quantum dots: emergent nanolights for bioimaging, sensors, catalysis and photovoltaic devices, *Chem. Commun.* 48 (2012) 3686–3699.
- [72] X. Zhou, Y. Zhang, C. Wang, X. Wu, Y. Yang, B. Zheng, H. Wu, S. Guo, J. Zhang, PhotoFenton reaction of graphene oxide: a new strategy to prepare graphene quantum dots for DNA cleavage, *ACS Nano* 6 (2012) 6592–6599.
- [73] Z. Zhang, J. Zhang, N. Chen, L. Qu, Graphene quantum dots: an emerging material for energy-related applications and beyond, *Energy Environ. Sci.* 5 (2012) 8869–8890.
- [74] X. Zhou, H. Pu, D.W. Sun, DNA functionalized metal and metal oxide nanoparticles: principles and recent advances in food safety detection, *Crit. Rev. Food Sci. Nutr.* 61 (14) (2021).
- [75] M. Hosseini, F. Khaki, E. Shokri, H. Khabbazi, M. Dadmehr, M.R. Ganjali, M. Feizabadi, D. Ajloo, Study on the interaction of the CpG Alternating DNA with CdTe quantum dots, *J. Fluoresc.* 27 (2017) 2059–2068.
- [76] M. Dadmehr, M. Hosseini, S. Hosseinkhani, M.R. Ganjali, M. Khoobi, H. Behzadi, M. Hamedani Sheikhejaei, DNA methylation detection by a novel fluorimetric anobiosensor for early cancer diagnosis, *Biosens. Bioelectron.* 60 (2014) 35–44.
- [77] S. Rafiei, M. Dadmehr, M. Hosseini, H. Ahmadzade Kermani, M.R. Ganjali, A fluorometric study on the effect of DNA methylation on DNA interaction with graphene quantum dots, *Methods Appl. Fluoresc.* 7 (2019) 025001.
- [78] M. Adampourezare, G. Dehghan, M. Hasanzadeh, M.A. Hosseinpoure Feizi, Identification of DNA methylation by novel optical genosensing: a new platform in epigenetic study using biomedical analysis, *J Mol Recognit* 34 (12) (2021) e2938.
- [79] M. Adampourezare, M. Hasanzadeh, G. Dehghan, M.A. Hosseinpoure Feizi, F. Seidi, An innovative fluorometric bioanalysis strategy towards recognition of DNA methylation using opto-active polymer: a new platform for DNA damage studies by genosensor technology, *J Mol Recognit* 35 (2022) 2981.
- [80] M.A. Karimi, M. Dadmehr, M. Hosseini, B. Korouzhdeh, F. Oroojalian, Sensitive detection of methylated DNA and methyltransferase activity based on the lighting up of FAM-labeled DNA quenched fluorescence by gold nanoparticles, *RSC Adv.* 9 (2019) 12063.